

## Removal of DBP from evening primrose oil with activated clay modified by chitosan and CTAB

FG Pan<sup>a</sup>, MQ Wang<sup>a</sup>, JY Xu<sup>a</sup>, CX Yang<sup>a</sup>, S Li<sup>a</sup>, YF Lu<sup>a</sup>, YD Zhang<sup>a</sup>, and BQ Liu<sup>a,✉</sup>

<sup>a</sup>Laboratory of Nutrition and Functional Food, College of Food Science and Engineering, Jilin University, Changchun 130062, PR China

✉Corresponding author: boqunliu@hotmail.com

Submitted: 7 April 2021; Accepted: 9 September 2021; Published online: 15 September 2022

**SUMMARY:** The pollution of phthalic acid esters (PAEs) in edible oils is a serious problem. In the current study, we attempt to remove dibutyl phthalate ester (DBP) from evening primrose oil (EPO) with modified activated clay. The activated clay, commonly used for de-coloration in the oil refining process, was modified by chitosan and hexadecyl trimethyl ammonium bromide (CTAB). The modifications were characterized by SEM, XRD, and FT-IR. We further tested the DBP adsorption capacity of CTAB/chitosan-clay and found that the removal rate was 27.56% which was 3.24 times higher than with pristine activated clay. In addition, the CTAB/chitosan-clay composite treatment had no significant effect on the quality of evening primrose oil. In summary, the CTAB/chitosan-clay composite has a stronger DBP adsorption capacity and can be used as a new adsorbent for removing DBP during the de-coloration process of evening primrose oil.

**KEYWORDS:** Activated clay; Evening primrose oil; Dibutyl phthalate ester.

**RESUMEN:** *Eliminación de DBP en aceite de onagra mediante arcilla activada modificada por chitosán y CTAB.* La contaminación por ésteres de ácido ftálico (PAEs) en los aceites comestibles es un problema grave. En el presente estudio, intentamos eliminar el éster de ftalato de dibutilo (DBP) del aceite de onagra (EPO) con arcilla activada modificada. La arcilla activada, comúnmente utilizada en la decoloración en el proceso de refinación de los aceites, fue modificada con chitosán y bromuro de hexadecil trimetil amonio (CTAB). Las modificaciones se caracterizaron mediante SEM, XRD y FT-IR. Además, probamos la capacidad de adsorción de DBP de CTAB / chitosán-arcilla y descubrimos que la tasa de eliminación era del 27,56%, que era 3,24 veces mayor que la arcilla activada pura. Además, el tratamiento compuesto de CTAB/chitosán-arcilla no tuvo un efecto significativo sobre la calidad del aceite de onagra. En resumen, el compuesto CTAB/chitosán-arcilla tiene una capacidad de adsorción de DBP más fuerte y se puede utilizar como un nuevo adsorbente para eliminar DBP durante el proceso de decoloración del aceite de onagra.

**PALABRAS CLAVE:** Aceite de onagra; Arcilla activada; Éster de ftalato de dibutilo.

**ORCID ID:** Pan FG, Wang MQ, Xu JY, Yang CX, Li S, Lu YF, Zhang YD, Liu BQ

**Citation/Cómo citar este artículo:** Pan FG, Wang MQ, Xu JY, Yang CX, Li S, Lu YF, Zhang YD, Liu BQ. 2022. Removal of DBP from evening primrose oil with activated clay modified by chitosan and CTAB. *Grasas y Aceites* 73 (3), e474. <https://doi.org/10.3989/gya.0438211>

**Copyright:** ©2022 CSIC. This is an open-access article distributed under the terms of the Creative Commons Attribution 4.0 International (CC BY 4.0) License.

## 1. INTRODUCTION

Phthalates, or phthalate esters, are esters of phthalic acid. They are mainly used as plasticizers in industry to produce hundreds of products including packaging materials, pharmaceuticals, blood bags and tubing, and personal care products (Kamrin, 2009; Net *et al.*, 2015; Giuliani *et al.*, 2020). PAEs are used primarily to soften polyvinyl chloride. PAEs are connected to polyvinyl chloride through intermolecular forces such as van der Waals forces or hydrogen bonds, which means PAEs can be released from the polymer and cause pollution to food, water, air, and soil (Gao and Wen, 2016). Studies have shown that PAEs have acute and chronic toxic effects on both aquatic organisms and terrestrial organisms (including humans) (Martino-Andrade and Chahoud, 2010; Benjamin *et al.*, 2017). Thus, many governments have issued relevant standards to limit PAE contents in products. The U.S. Environmental Protection Agency has included 6 types of PAEs in the list of priority pollutants, and the European Union, Japan and China have their own standards to limit the content of PAEs in products (Zhang *et al.*, 2015).

Phthalates are characterized as highly soluble in fat, so food products containing a higher fat content are more likely to contain higher levels of phthalate (Liu *et al.*, 2020). Researchers have already evaluated the pollution level of PAEs in edible oils in various countries and regions (Kong *et al.*, 2022; Xiang *et al.*, 2019; Zhao *et al.*, 2014). Wei *et al.* (2020) collected 1016 samples of edible oil blends, soybean oil, peanut oil and rapeseed oil from all over China. They found 13.48% of the samples contained DBP, while 7.78% of the samples contained DEHP. Similar work was also done by Bi *et al.* (2013). They tested the content of PAEs in 21 edible vegetable oil samples which were collected from the US market. About 90.5% of the samples contained DBP and all the samples contained DEHP. Moreover, the highest concentration in DBP was 95.8  $\mu\text{g}/\text{kg}$ , while the highest concentration in DEHP was 6166  $\mu\text{g}/\text{kg}$ . The high concentration in bis(2-ethylhexyl) phthalate (DEHP) in oil is higher than the maximum residual levels which set by the Chinese Government (1.5 mg/kg), (Pereira *et al.*, 2019). Thus, DBP and DEHP in oil should be removed.

However, the current research on the removal of PAEs in oil is relatively simple (Kotowska *et al.*,

2020; Pang *et al.*, 2021). Adsorption, steam distillation and molecular distillation are the three most widely investigated methods. Among them, molecular distillation has the highest removal efficiency of PAEs, generally up to 90% or more (Chen *et al.*, 2019; Xiong *et al.*, 2013; Gelmez *et al.*, 2017), but this method is difficult to be widely used due to its high cost and difficulties in industrialization. Adsorption and steam distillation are widely used in the refining process of de-coloration and deodorization processes in edible oil. Some researchers have reported that steam distillation has a certain ability to remove PAEs. Chen *et al.* (2019) successfully removed 82% of DBP and 66% of DEHP in sea buckthorn fruit oil with two consecutive steam distillation treatments. In our work, we applied steam distillation to the refining process of evening primrose oil. We found significant differences in different batches. That is, in a certain batch, the PAE can be removed successfully. However, in another batch nearly no PAEs could be removed. We cannot solve this problem at present. Hence, we referred to the adsorption method. The adsorbents (activated carbon, activated clay, attapulgite and diatomite) commonly used in the oil refining process have very little adsorption capacity for PAEs. Therefore, a novel type of adsorbent, which is low in cost and easy to operate is needed for removing PAEs from evening primrose oil.

Activated clay is the most commonly used adsorbent in the de-coloration process of edible oil (Zhang *et al.*, 2021). There are some studies that have shown that after modification with CTAB and chitosan, the adsorption capacity of activated clay can be greatly increased. Cao *et al.* (2014) used CTAB to organically modify Na-bentonite. The results of XRD and BET showed that the pore size and interlayer spacing of bentonite became larger after modification, and the removal rate of phenol in water by modified clay could reach 81.36%. Rahardjo *et al.* (2011) prepared CTAB modified bentonite. XRD and FT-IR results showed that CTAB was successfully inserted between the layers so that the distance between the bentonite layers became larger, that the surface structure changed to a certain extent, and that the affinity for hydrophobic substances became stronger. Compared to unmodified bentonite, modified bentonite exhibited stronger adsorption capacity for organic matter and heavy

metal ions. Guo *et al.* (2012) prepared a chitosan/CTAB combined modified activated clay. After modification, the adsorption efficiency of the clay on the weakly-acidic scarlet dye could reach up to 85%. Therefore, in the current work, we prepared a CTAB/chitosan-clay composite. Then we studied the surface characteristics of the adsorbent and the adsorption capacity of DBP in evening primrose oil (EPO), and investigated the effect of CTAB/chitosan-clay composite treatment on the quality of EPO. At the same time, the adsorption mechanism of the CTAB/chitosan-clay composite to adsorb DBP in EPO was determined.

## 2. MATERIALS AND METHODS

### 2.1. Materials

Evening primrose oil (EPO) was collected from the Baili Biotech Company in Changchun, Jilin, China. Activated Clay was purchased from a Chinese market (Decolorization rate  $\geq 98\%$ , Activity  $\geq 100$  mmol/kg, free acid content  $\leq 0.5\%$ , moisture content  $\leq 12.0\%$ ). CTAB (purity  $\geq 98\%$ ) and chitosan (Viscosity = 50-100 mpa, 95% degree of deacetylation) were purchased from Roche. Standard dibutyl phthalate ester was purchased from Aladdin, China. The chemical reagents involved in GC-MS detection were of chromatographic purity (purchased from CNW, Germany). All other chemical reagents (including solvents) were of analytical grade and purchased from local suppliers. Water was purified by the Milli-Q water purification system (Millipore, Bedford, USA).

### 2.2. Synthesis of CTAB/chitosan-clay composite

The CTAB/chitosan-clay composite was prepared in the ratio chitosan: CTAB: clay = 0.2:0.3:1. The chitosan (2 g) was dissolved in a 300 mL 3% acetic acid solution, and stirred at 60 °C in a temperature-controlled water bath until the chitosan was completely dissolved. Then the chitosan solution was mixed with 10 g activated clay and 3 g CTAB. The mixture was again subjected to moderate stirring in a temperature-controlled water bath at 60 °C for 6 h. The mixtures were centrifuged and washed with deionized water. The wet mixture was dried at 80 °C for 48 h. After the formation of CTAB/chitosan-clay, the composite was sieved to obtain a powder.

### 2.3. Characterization techniques of CTAB/chitosan-clay composite

The preparation of CTAB/chitosan-clay composite was verified by a series of characterization methods. The surface morphologies of the pristine activated clay and CTAB/chitosan-clay composite were determined by scanning electron microscope (SEM, ZEISS Gemini SEM500), with 2-3 kV working voltage and 10-100 K magnification, by spraying gold-plated palladium alloy onto the sample surface before testing. CTAB/chitosan-clay composite and pristine activated clay were recorded on a powder X-ray diffractometer (XRD, Smartlab 9 kW, operating at 40 kV). The CuK $\alpha$  radiation source with a wavelength of 1.54 Å was used and the data was collected for a wide-angle region ranging between 5 and 80° on a 2 $\theta$  scale with a scan rate of 5°/min. The surface area of the composite was measured by BET measurements, using a Micromeritics ASAP 2020 instrument at liquid nitrogen temperature (77 K) via nitrogen gas adsorption. The Fourier-transformed infrared (FT-IR) spectra of the CTAB/chitosan-clay composite and chitosan and pristine activated clay were recorded on an IR Prestige-21 FTIR in KBr pellets. The detailed work is shown in a former paper.

### 2.4. Methodology for adsorption of DBP in EPO

Adsorption experiments were carried out in batch mode in a temperature-controlled water bath with constant stirring under vacuum. The removal rate of DBP in oil was determined and the adsorption efficiency was calculated as:

$$\text{Adsorption efficiency (\%)} = \frac{C_0 - C_e}{C_0} * 100\%$$

Where  $c_0$  and  $c_e$  (mg/kg) are the initial and equilibrium concentrations of DBP in the reaction medium. Adsorption kinetics were obtained by treating 2 g of CTAB/chitosan-clay composite with 20 g EPO of 10 mg/kg DBP of initial concentration in the time range 0-540 min under optimized adsorption conditions. The adsorption isotherms were obtained by treating 2 g of CTAB/chitosan-clay composite with 20 g EPO of DBP of initial concentration in the range of 1-25 mg/kg under optimized adsorption conditions.

## 2.5. DBP composition analysis in EPO by GC-MS

Oil sample preparation was performed according to Chinese national standard GB 5009.271-2016. DBP determination was performed using a Shimadzu GC-MS QP-2010 Ultra. A Rxi-5MS column (30 m × 0.25 mm × 0.25 μm) was from Shimadzu Inc. Oven temperature was set initially at 60 °C for 1 min, programmed to increase at 20 °C/min to 220 °C and held for 1 min, then increased to 250 °C at 5 °C/min, held for 1 min and then increased to 290 °C at 20 °C/min, the temperature was then maintained for 6 min. Helium (99.999% purity) was used as a carrier gas at a constant flow rate of 1.0 mL/min and the injection volume was 1 μL. The injector, transfer and ion source temperatures, were set at 260, 230 and 280 °C, respectively. EI was used as the electron bombardment ion source and the ionization energy was 70 eV. Scan mode (Scan) was used for qualitative and selective ion monitoring and (SIM) was used for the quantitative analysis. The qualifier ion of DBP was 91, 206, 238(m/z), while the quantitative ion was 149 (m/z).

## 2.6. Analysis of physicochemical properties of evening primrose oil

The peroxide value (POV) was determined according to Chinese national standard GB 5009.227-2016 and the results were expressed as millimole (mmol)/kg of oil. The acid value (AV) was measured according to Chinese national standard GB/T 5009.229-2016 and expressed in mg KOH/g. The iodine value (IV) was evaluated by reference to Chinese national standard GB/T 5532-2008. The *p*-anisidine value (*p*-AV) was measured by Chinese national standard GB/T 24304-2009.

## 2.7. Analysis of fatty acid composition

The fatty acid composition was determined according to the method proposed by Pan *et al.* (2020) with few modifications. Briefly, 100 mg (accurate to 0.1 mg) EPO were mixed with 2 mL of *n*-heptane and 2 mL of 2 M KOH-methanol, and shaken vigorously until well mixed. After the mixture was allowed to stand for stratification, the supernatant was taken out, and an appropriate amount of anhydrous Na<sub>2</sub>SO<sub>4</sub> was added to remove the water. Finally, after passing the mixture through a 0.22 μm organic filter membrane, the supernatant could be

analyzed. Samples were subjected to a Shimadzu GC-MS QP2010Ultra and a Rxi-5MS column (30 m × 0.25 mm × 0.25 μm). The oven temperature was set at an initial temperature of 160 °C, held for 5 min, then increased at 2 °C/min to 220 °C, held for 10 min, programmed to increase at 4 °C/min to 240 °C with a final holding time of 10 min. Helium (99.999% purity) was used as carrier gas in a constant flow of 1.0 mL/min and the injection volume was 1 μL, with an AOC-20i autosampler split ratio of 1:50. The temperatures of injector, transfer and ion source were set at 260, 200 and 250 °C, respectively. The ionization energy was 70 eV and the change in total ion current in the range of m/z 50-500 was recorded. Fatty acids were identified by comparison with data and the NIST Mass Spectrometry Library (National Institute of Standards and Technology, Gaithersburg, MD, USA). The results were recorded across the percentage of the relative peak areas.

## 2.8. Statistical analysis

The samples were measured in triplicate, and the results were expressed as mean ± standard deviation (SD).

## 3. RESULTS AND DISCUSSION

### 3.1. Characterization of the CTAB/chitosan-clay composite

The SEM results clearly indicated that the surface morphology of clay changed after modification. As shown in Figure 1(a), the pristine activated clay showed a typical agglomerated flake structure. The surface of unmodified clay was relatively smooth, flat and compact. On the contrary, the CTAB/chitosan-clay composite had a heavier curling degree at the edge, and with a looser interlayer structure and rougher surface. The looser interlayer structure could increase the diffusion of PAEs into the CTAB/chitosan-clay composite (Alshameri *et al.*, 2018). These characters changed together mean that more functional groups might be exposed to the environments and the functional group could interact with PAE more efficiently. Thus, the modified clay could remove the DBP from evening promise oil more efficiently.

The absorption peak positions of pristine activated clay before and after modification were

basically the same according to the XRD results (Figure 1(b)). The results indicated that the addition of CTAB and chitosan did not change the basic structure, which is an agglomerated flake structure, of activated clay. The main changes after modification might refer to the looser interlayer structure. According to previous research, the silicate group in the pristine activated clay may interact with the hydroxyl group of chitosan by hydrogen bonding. Thus, the silicate group played the role of an anchor and held the chitosan (Mohd *et al.*, 2018). The silicate group in the pristine activated clay was considered to remain constant while the long carbon chain of CTAB was directly inserted between the layers of the pristine activated clay. The position of the characteristic diffraction peak of  $d(001)$  existing in the clay close to  $2\theta=5^\circ$  shifted to the left. From the Bragg equation ( $2d\sin\theta=n\lambda$ ), it could be seen that the layer spacing of pristine activated clay increased after modification. In addition, the material composition analysis of the XRD structure showed that the main components of the adsorbent before and after the modification were basically the same, which were quartz, albite and illite.

Furthermore, the Brunauer-Emmett-Teller (BET) surface area of the pristine activated clay was measured as  $137.0916\text{ m}^2/\text{g}$ , while the BET surface area of the CTAB/chitosan-clay composite was  $18.4283\text{ m}^2/\text{g}$ . Furthermore, the pore volume of the pristine activated clay was determined to be  $0.1909\text{ cm}^3/\text{g}$ , and the CTAB/chitosan-clay composite's pore volume was  $0.0843\text{ cm}^3/\text{g}$ . The decrease in the surface area and pore volume was attributable to the intercalation of CTAB and chitosan molecules in the interlayers of pristine activated clay which resulted in the pore blockage (Budyak *et al.*, 2016; Zhang *et al.*, 2009). However, CTAB/chitosan-clay composite ( $15.9528\text{ nm}$ ) had a larger pore size than pristine activated clay ( $6.6768\text{ nm}$ ). Pore size influences the behavior of the adsorbate-adsorbent system (Wang *et al.*, 2020). A suitable size of pore may help in the absorptions process.

The FT-IR (Figure 1(c)) of chitosan, pristine activated clay and CTAB/chitosan-clay composite revealed the changes in the functional groups in the composite. The peak shape of the infrared spectrum of the activated clay before and after modification did not change significantly, and the characteristic absorption peaks of the activated clay

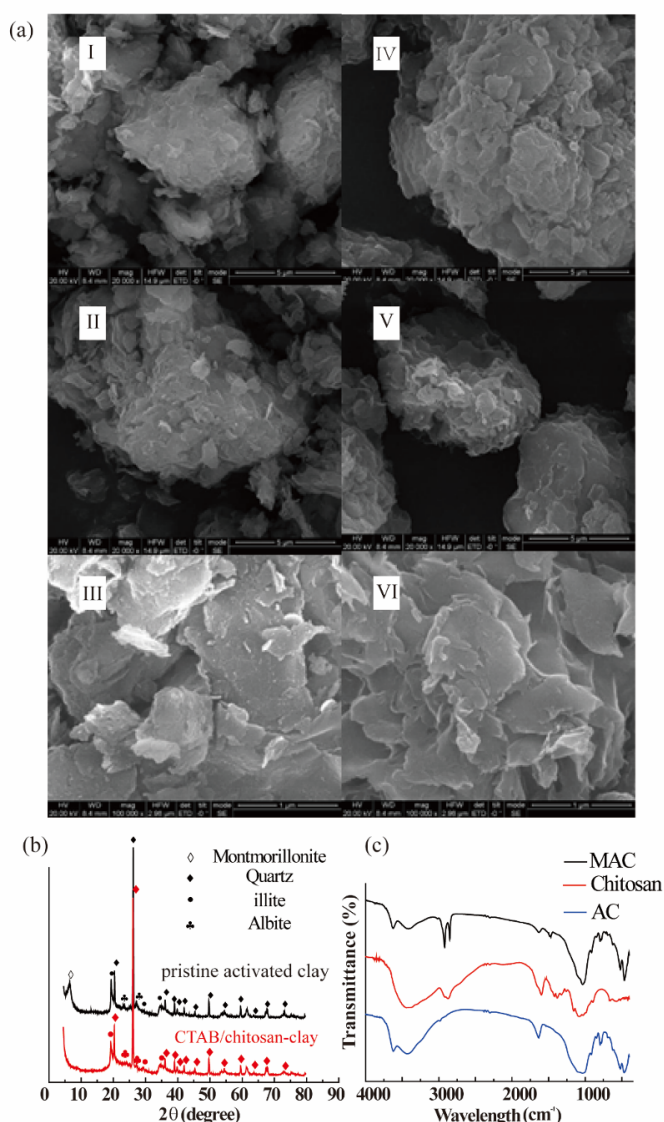


FIGURE 1. Characterization test results of activated clay and CTAB/chitosan-clay composite: (a)SEM(I, II, III for activated clay and IV, V, VI for CTAB/chitosan-clay composite), (b)XRD, (c)FT-IR.

appeared, indicating that the modification did not change the typical agglomerated flake structure of the activated clay, which was consistent with the XRD results. There were four new peaks at  $2920\text{ cm}^{-1}$ ,  $2850\text{ cm}^{-1}$ ,  $1482\text{ cm}^{-1}$  in CTAB/chitosan-clay composite. The peaks at  $2920\text{ cm}^{-1}$  and  $2850\text{ cm}^{-1}$  were asymmetric and symmetric stretching vibration peaks of CTAB's and chitosan's  $-\text{CH}-$ , respectively. The peak at  $1482\text{ cm}^{-1}$  was a symmetric bending vibration of  $-\text{CH}-$ , which was detected at  $1443\text{ cm}^{-1}$  in original activated clay (Fu *et al.*, 2017). These results indicated that there were certain interactions between the CTAB, chitosan and activated clay.

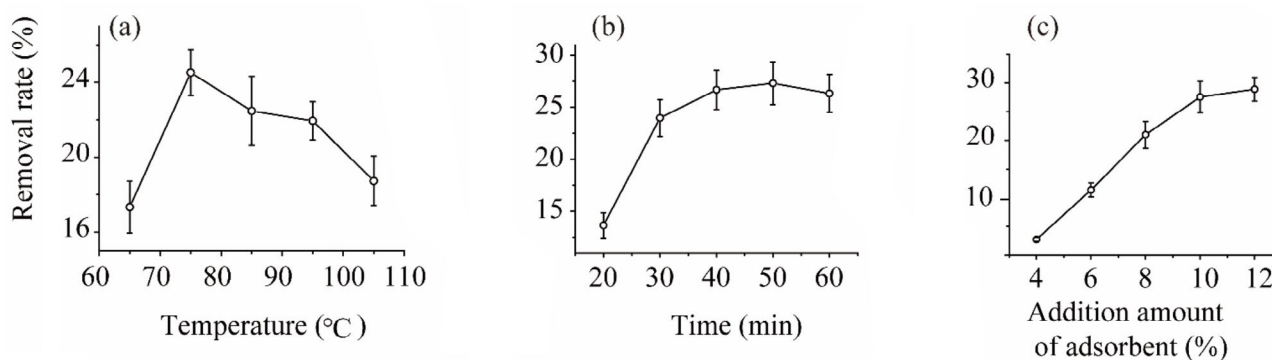


FIGURE 2. Effect of (a) temperature, (b) time, (c) adsorbent doses (% Madsorbent/MEPO) on adsorption efficiency of DBP in evening primrose oil, initial concentration of DBP=2 mg/kg, weight of evening primrose oil=20 g. Each value in the figure represents the mean  $\pm$  SD ( $n=3$ ).

### 3.2. The optimization of adsorption conditions

To optimize the parameters for removing DBP from EPO, we investigated the influence of temperature, time and the additional amount of adsorbent on the adsorption. The entire adsorption was carried out under vacuum conditions. The adsorption results are shown in Figure 2.

The influence of temperature is shown in Figure 2(a). The adsorption rate of DBP could be increased from 17.33 to 24.52% when the temperature increased from 65 to 75 °C. However, when the temperature ranged from 75 to 105 °C, the adsorption rate of DBP showed a downward trend. This might be due to the higher temperature accelerating the resolution of DBP on the adsorbent, resulting in a decrease in its adsorption rate. Hence, the optimal temperature was chosen as 75 °C. The influence of time is shown in Figure 2(b). When the adsorption time increased from 20 to 40 min, the adsorption rate of DBP increased rapidly from 14 to 28%. After that, the adsorption rate slowed down and fluctuated at 30%. Hence, considering the efficiency, the optimal time was chosen as 40 min. Similar trends were found in the adsorbent dose. As shown in Figure 2(c), the adsorption rate of DBP increased with the increase in adsorbent dose. How-

ever, when the amount of adsorbent added exceeded 10% (w/w), the growth of DBP adsorption efficiency slowed down significantly. This might be because too much adsorbent would reduce the adsorption capacity per unit mass of adsorbent and affect the utilization rate of the adsorbent. Hence, the optimal amount of adsorbent was chosen as 10%. In short, under the optimal conditions described above, the adsorption rate of the adsorbent to DBP was 27.56%, while the removal rate of pristine activated clay was only 8.51% under the same conditions.

### 3.3. The change in the properties of evening primrose oil

The physical and chemical properties of evening primrose oil treated by activated clay (named as AC-EPO) and CTAB/chitosan-clay composite (named as MAC-EPO) were determined under the same conditions. The physical and chemical indicators of evening primrose oil processed with different clay are shown in Table 1. There were no significant differences in acid value, peroxide value, or *p*-AV, among AC-EPO and MAC-EPO, and iodine value.

The *p*-AV can be used to measure the number of secondary products such as aldehydes, ketones, and

TABLE 1. Comparison of the quality of evening primrose oil treated by activated clay and CTAB/chitosan-clay composite

|         | AV (KOH)<br>mg/g | POV<br>mmol/kg | IV<br>g·100g <sup>-1</sup> | <i>p</i> -AV | C16:0<br>(%) | C18:0<br>(%) | C18:1<br>(%) | C18:2<br>(%) | C18:3n3<br>(%) | C18:3n6<br>(%) |
|---------|------------------|----------------|----------------------------|--------------|--------------|--------------|--------------|--------------|----------------|----------------|
| AC-EPO  | 0.38±0.04a       | 1.38±0.09b     | 163.22±2.19c               | 6.22±0.24d   | 8.6±0.09e    | 2.89±0.09f   | 5.77±0.21g   | 71.27±0.39h  | 0.30±0.03i     | 9.73±0.18j     |
| MAC-EPO | 0.40±0.02a       | 1.29±0.07b     | 161.01±1.48c               | 7.68±0.14d   | 8.52±0.16e   | 2.9±0.07f    | 6.37±0.32g   | 70.45±0.46h  | 0.47±0.02i     | 9.52±0.21j     |

Each value in the table represents the mean  $\pm$  SD ( $n=3$ ). AV: Acid value, POV: Peroxide value, IV: Iodine value, *p*-AV: *p*-Anisidine value. Letters in the same column indicate the significance of evening primrose oil treated by different adsorbent: the same letters represent no significant difference ( $p > 0.05$ ), and different letters represent significant difference ( $p < 0.05$ ), compared by ANOVA (Tukey-Kramer HSD test).

quinones in the oil. In the oil refining process, the *p*-AV value of the oil in the decolorization process can be the highest. This is because the clay can catalyze the decomposition of hydroperoxides to generate aldehydes and ketones (Kreps *et al.*, 2014). The CTAB/chitosan-clay had a stronger catalytic ability to hydroperoxide in oil, which increased the contents in aldehydes and ketones, and finally made the *p*-AV value of MAC-EPO higher than AC-EPO.

AV is an important indicator of oil quality, and IV is the response to the degree of unsaturation of oils. The AV of AC-EPO and MAC-EPO were both around 0.4, while the IV in MAC-EPO dropped slightly. This might be due to insufficient vacuum during the adsorption process, so some unsaturated fatty acids were oxidized.

### 3.4. Comparison between the fatty acid compositions of evening primrose oil with different treatments

The main fatty acids contained in EPO are  $\alpha$ -linolenic acid,  $\gamma$ -linolenic acid, linoleic acid, oleic acid, stearic acid and palmitic acid, which can reach more than 98% (Zhao *et al.*, 2019). Linoleic acid (C18:2) is the major fatty acid in EPO, which can reach more than 70%.  $\gamma$ -linolenic acid (C18:3n6), which is a characteristic nutrient of evening primrose oil, and its content is required to be above 9%. Table 1 lists the fatty acid contents in AC-EPO and MAC-EPO, respectively. The fatty acid composition of AC-EPO and MAC-EPO was not significantly different. The total amount of 5 fatty acids in AC-EPO was 98.56% and the amount of unsaturated fatty acids (UFA) was 87.07%, while the total amount of 5 fatty acids in MAC-EPO reached 98.23% and the amount of UFA was 86.81%. Therefore, the CTAB/chitosan-clay composite adsorption treatment had almost no effect on the fatty acid composition of EPO.

### 3.5. Adsorption kinetics

The adsorption kinetics test was performed. 10 mg/kg DBP were added to the evening primrose oil and the amount of DBP was recorded over time. The residual concentration of DBP and the interaction time of the CTAB/chitosan-clay composite adsorption treatment was plotted. The results are shown in Figure 3. It can be seen that the adsorption amount of DBP by the CTAB/chitosan-clay composite material increased with the increase in contact time, to reach an equilib-

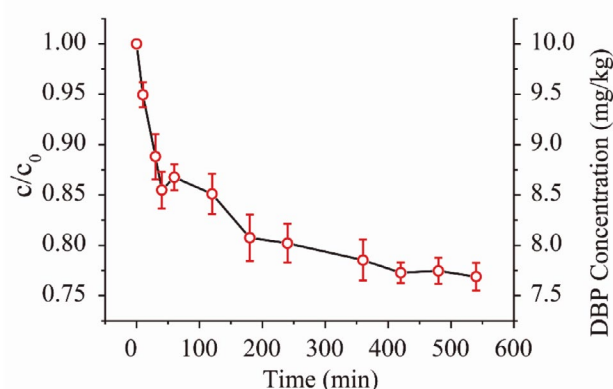


FIGURE 3. Changes in the remaining concentration of DBP in evening primrose oil over time. Adsorption kinetics were obtained by treating 2 g of CTAB/chitosan-clay composite with 20 g evening primrose oil of  $c_0=10$  mg/kg DBP of initial concentration in the time range 0-540 min under optimized adsorption conditions.  $c$  was the concentration of DBP at time  $t$ .

rium state at about 420 minutes. We employed two kinetic models, pseudo-first-order and pseudo-second-order kinetic models, to study the adsorption process of DBP on CTAB/chitosan-clay composite. The pseudo-first-order kinetic model is represented by the following formula (Mohd *et al.*, 2018):

$$\log(q_e - q_t) = \log q_e - \frac{k_1}{2.303} t$$

$$q_e = \frac{c_0 - c_e}{m_{adsorbent}} * m_{EPO}$$

The pseudo-second-order kinetic model is represented as (Mohd *et al.*, 2018):

$$\frac{t}{q_t} = \frac{1}{k_2 q_e^2} + \frac{t}{q_e}$$

Where  $k_1$  and  $k_2$  are the rate constants of the pseudo-first-order and pseudo-second-order adsorption kinetic equations.  $c_0$  and  $c_e$  are the initial concentration and equilibrium concentration of DBP, respectively.  $q_e$  and  $q_t$  are the adsorption capacity of the adsorbent in equilibrium and at time  $t$ , respectively. The slope and intercept of the  $\log(q_e - q_t)$  versus  $t$  and  $t/q_t$  versus  $t$  curves were used to derive  $k_1$  and  $k_2$ , respectively.

Figure 4 shows the linear fitting of two kinetic models, and the parameters obtained after fitting are listed in Table 2. The linear regression coefficient value of the pseudo-second-order kinetic model was

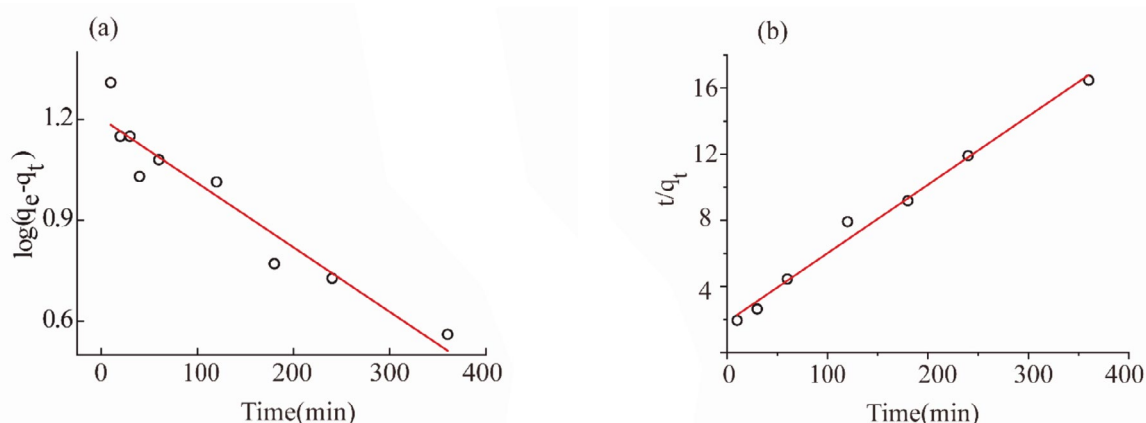


FIGURE 4. Adsorption kinetics of DBP in the CTAB/chitosan-clay composite fitted with (a) pseudo-first-order model; (b) pseudo-second-order model. Adsorption kinetics were obtained by treating 2 g of CTAB/chitosan-clay composite with 20 g evening primrose oil of  $c_0=10$  mg/kg DBP of initial concentration in the time range 0-540 min under optimized adsorption conditions.

higher ( $R^2=0.9902$ ), which could better describe the adsorption of DBP on CTAB/chitosan-clay composite. The pseudo-second-order kinetic model assumes that the rate-limiting step is chemical sorption or chemisorption and predicts the behavior over the whole range of adsorption (Bujdák, 2020). In other words, the adsorption rate is dependent on adsorption capacity and not on the concentration of adsorbate. Thus, the future research should focus on the modification of clay and increase the adsorption capacity of the clay. In addition, the  $q_e$  value obtained by the pseudo-second-order kinetic model was closer to the  $q_e$  value obtained from the experiment. Furthermore, the pseudo-second-order kinetic model favors the chemisorption concerning valency forces through the sharing or exchanging of electrons between adsorbent and adsorbate. Hence, the results indicate that there might be an electron exchange between the adsorbent and the adsorbate (Ho *et al.*, 2006). The chitosan and CTAB are typical positive molecules, while the dibutyl phthalate esters are negative. The electrostatic interactions between them may contribute during absorptions.

### 3.6. Adsorption isotherms

The adsorption isotherm curve is the relationship curve of the concentration of the reaction solute molecules in the two phases when the adsorption process reaches equilibrium at a certain temperature. The DBP adsorption on CTAB/chitosan-clay composite was studied with Langmuir and Freundlich adsorption isotherm models. The initial concentrations of the DBP ( $c_0$ ) in evening primrose oil were taken in the range of 1-25 mg/kg. Determined the equilibrium concentration of DBP ( $c_e$ ), and the  $q_e$  value of the adsorbent. The linear Freundlich adsorption isotherm model is represented by the following formula (Acikyildiz *et al.*, 2015):

$$\log q_e = \log K_F + \frac{1}{n} \log c_e$$

Among them,  $K_F$  and  $n$  are Freundlich isothermal constants, which are related to adsorption capacity and strength, respectively. Usually, it is considered that the reaction conditions are conducive to the pro-

TABLE 2. Adsorption capacity and adsorption kinetics for DBP sorption by CTAB/chitosan-clay fitted with pseudo first order and pseudo second order models

| Sample             | $q_{e,exp}$<br>(mg/kg) | Pseudo first order kinetic      |                                |        | Pseudo second order kinetic     |                                |        |
|--------------------|------------------------|---------------------------------|--------------------------------|--------|---------------------------------|--------------------------------|--------|
|                    |                        | $q_{1e}$<br>( $\mu\text{g/g}$ ) | $k_1$<br>( $\text{min}^{-1}$ ) | $R^2$  | $q_{2e}$<br>( $\mu\text{g/g}$ ) | $k_2$<br>( $\text{min}^{-1}$ ) | $R^2$  |
| CTAB/chitosan-clay | 25.51                  | 16.08                           | 0.005                          | 0.9143 | 24.10                           | 0.001                          | 0.9902 |

$k_1$  and  $k_2$  are the rate constants of the pseudo-first-order and pseudo-second-order adsorption kinetic equations.  $q_e$  and  $q_{e,exp}$  are the adsorption capacity of the adsorbent in equilibrium in theory and reality, respectively.

TABLE 3. Adsorption isotherm parameters for DBP sorption by CTAB/chitosan-clay composite

| Langmuir parameters |                          |                | Freundlich parameters |                |      |
|---------------------|--------------------------|----------------|-----------------------|----------------|------|
| R <sup>2</sup>      | q <sub>m</sub><br>(μg/g) | K <sub>L</sub> | R <sup>2</sup>        | K <sub>F</sub> | n    |
| 0.9307              | 73.53                    | 0.033          | 0.9886                | 2.16           | 1.13 |

K<sub>F</sub> and n are Freundlich isothermal constants and K<sub>L</sub> is the constant of the Langmuir equation. q<sub>m</sub> is the theoretical maximum adsorption capacity of DBP derived from the Langmuir equation.

gress of adsorption when n>1. Values of K<sub>F</sub>, n and R<sup>2</sup> are given in Table 3.

The linear Langmuir adsorption isotherm model is represented as (Acikyildiz *et al.*, 2015):

$$\frac{c_e}{q_e} = \frac{1}{q_m K_L} + \frac{c_e}{q_m}$$

The equilibrium parameter, R<sub>L</sub> is evaluated as:

$$R_L = \frac{1}{1 + (1 + K_L c_o)}$$

Where q<sub>m</sub> (μg/g) is the theoretical maximum adsorption capacity of the adsorbent. K<sub>L</sub> is the constant of the Langmuir equation. R<sub>L</sub> is the dimensionless constant separation factor. When 0 < R<sub>L</sub> < 1, the adsorption process is preferential adsorption. The K<sub>L</sub>, q<sub>m</sub> and R<sup>2</sup> values are given in Table 3.

In Figure 5, the correlation coefficients R<sup>2</sup> of Langmuir and Freundlich were both above 0.9,

which were 0.9307 and 0.9886, respectively. This indicated that the adsorption process was dominated by monolayer adsorption, which might include physical and chemical adsorption. Similarly, the value of R<sub>L</sub> (between 0.35 and 0.5) and the value of n (n > 1) also showed a favorable adsorption process.

#### 4. CONCLUSIONS

In this study, we modified the activated clay modified by chitosan and CTAB and applied this composite for the absorption of DBP in evening primrose oil. We optimized the absorption conditions for this CTAB/chitosan-clay composite. When the amount of CTAB/chitosan-clay composite, temperature and time were 10%, 75 °C, and 40 min, respectively, the maximum adsorption rate of the adsorbent to DBP was 27.56%, which is 3.24 times higher than the adsorption efficiency of pristine activated clay. In addition, we tested the physicochemical properties and fatty acid composition of evening primrose oil treated with activated clay and CTAB/chitosan-clay. The results indicate that the modification did not influence evening primrose oil, which indicated that the CTAB/chitosan-clay could be applied in the industry.

We also investigated the possible mechanism of the absorptions of the CTAB/chitosan-clay composite. According to the SEM and XRD, we found that the specific surface area and pore volume of the CTAB/chitosan-clay composite were reduced, while the pore diameter and interlayer spacing became larger. This phenomenon may be due to the loading of functional groups to the clay. The larg-

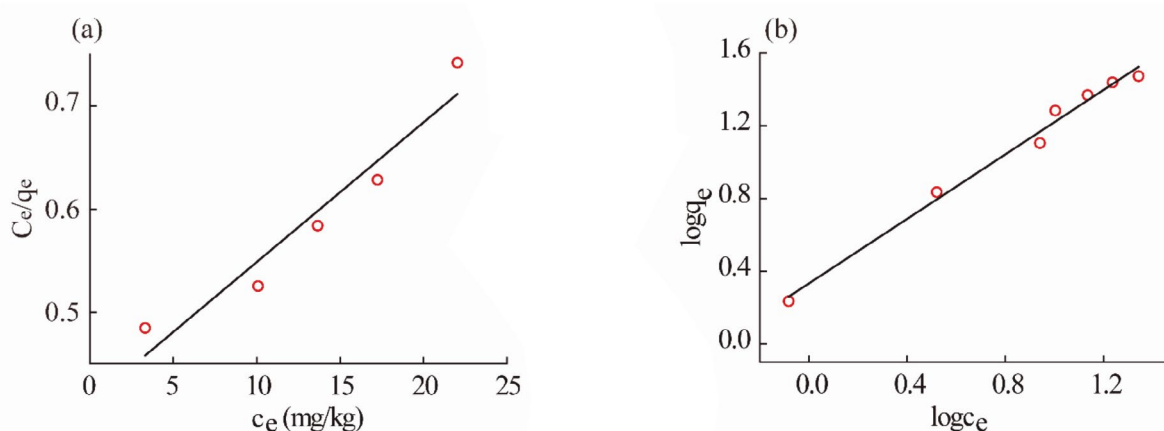


FIGURE 5. Adsorption isotherms of DBP in CTAB/chitosan-clay composite linearly fitted by: (a) Langmuir adsorption isotherm; (b) Freundlich adsorption isotherm. Adsorption isotherms were obtained by treating 2 g of CTAB/chitosan-clay composite with 20 g evening primrose oil and the initial DBP concentrations ranged between c<sub>0</sub> = 1 and 25 mg/kg, under optimized adsorption conditions.

er pore size and interlayer spacing could help in the diffusion DBP in the CTAB/chitosan-clay composite. We also performed the absorption kinetic of the CTAB/chitosan-clay composite. The kinetic results showed that the pseudo-second-order kinetic model better described the adsorption process of DBP in the CTAB/chitosan-clay composite. The thermodynamic analysis showed that the Freundlich model more accurately described the adsorption process of DBP in the CTAB/chitosan-clay composite, and the value of  $R_L$  (from Langmuir model, between 0 and 1) and the value of  $n$  (from Freundlich model,  $n > 1$ ) showed a favorable adsorption process. The results of the kinetics and thermodynamic analyses indicated that adsorption was dominated by monolayer adsorption, and electrostatic forces and the hydrogen bonding forces contributed most during the absorption. In conclusion, the CTAB/chitosan clay composite can be a new choice of adsorbent that can be used in the de-coloration process of evening primrose oil.

#### ACKNOWLEDGMENTS

The authors would like to express gratitude to the financial support provided by the Program for Jilin Province science and technology development project (No. 20190301058NY).

#### REFERENCES

- Acikyildiz M, Gurses A, Gunes K, Yalvac D. 2015. A comparative examination of the adsorption mechanism of an anionic textile dye (RBY 3GL) onto the powdered activated carbon (PAC) using various the isotherm models and kinetics equations with linear and non-linear methods. *Surf. Sci.* **354**, 279–284. <https://doi.org/10.1016/j.apsusc.2015.07.021>
- Alshameri A, He H, Zhu J, Xi Y, Zhu R, Ma L, Tao Q. 2018. Adsorption of ammonium by different natural clay minerals: characterization, kinetics and adsorption isotherms. *Appl. Clay Sci.* **159**, 83–93. <https://doi.org/10.1016/j.clay.2017.11.007>
- Benjamin S, Masai E, Kamimura N, Takahashi K, Anderson RC, Faisal PA. 2017. Phthalates impact human health: epidemiological evidences and plausible mechanism of action. *J. Hazard. Mater.* **340**, 360–383. <https://doi.org/10.1016/j.jhazmat.2017.06.036>
- Bujdák J. 2020. Adsorption kinetics models in clay systems. The critical analysis of pseudo-second order mechanism. *Appl. Clay Sci.* **191**, 105630. <https://doi.org/10.1016/j.clay.2020.105630>
- Bi XL, Pan XJ, Yuan SJ. 2013. Plasticizer Contamination in Edible Vegetable Oil in a U.S. Retail Market. *J. Agric. Food Chem.* **61**, 9502-9509. <https://doi.org/10.1021/jf402576a>
- Budyak TM, Yanovska ES, Kichkiruk OY, Sternik D, Tertykh VA. 2016. Natural minerals coated by biopolymer chitosan: synthesis, physicochemical and adsorption properties. *Nanoscale Res. Lett.* **11**, 492. <https://doi.org/10.1186/s11671-016-1696-y>
- Cao C, Meng L, Zhao Y. 2014. Adsorption of phenol from wastewater by organo-bentonite. *Desalin. Water Treat.* **52**, 19-21. <https://doi.org/10.1080/19443994.2013.803649>
- Chen L, Liu Y, Deng J. 2019. Removal of phthalic acid esters from sea buckthorn (*Hippophae rhamnoides* L.) pulp oil by steam distillation and molecular distillation. *Food Chem.* **294**, 572-577. <https://doi.org/10.1016/j.foodchem.2019.05.091>
- Fu L, Yang H, Tang A, Hu Y. 2017. Engineering a tubular mesoporous silica nanocontainer with well-preserved clay shell from natural halloysite. *Nano Res.* **10** (8), 2782-2799. <https://doi.org/10.1007/s12274-017-1482-x>
- Gao DW, Wen ZD. 2016. Phthalate esters in the environment: A critical review of their occurrence, biodegradation, and removal during wastewater treatment processes. *Sci. Total Environ.* **541**, 986-1001. <https://doi.org/10.1016/j.scitotenv.2015.09.148>
- Gelmez B, Ketenoglu O, Yavuz H. 2017. Removal of di-2-ethylhexyl phthalate (DEHP) and mineral oil from crude hazelnut skin oil using molecular distillation-multiobjective optimization for DEHP and tocopherol. *Eur. J. Lipid Sci. Technol.* **116**, 1600001. <https://doi.org/10.1002/ejlt.201600001>
- Giuliani A, Zuccarini M, Cichelli A, Khan H, Reale M. 2020. Critical review on the presence of phthalates in food and evidence of their biological impact. *International Int. J. Environ. Res. Public Health*, **17** (16), 5655. <https://doi.org/10.3390/ijerph17165655>
- Guo J, Chen S, Liu L. 2012. Adsorption of dye from wastewater using chitosan-CTAB modified bentonites. *J. Colloid Interface Sci.* **382**, 61-66. <https://doi.org/10.1016/j.jcis.2012.05.044>
- Ho YS. 2006. Review of second-order models for adsorption systems. *J. Hazard. Mater.*

- 136(3), 681-689. <https://doi.org/10.1016/j.jhazmat.2005.12.043>
- Kamrin MA. 2009. Phthalate Risks, Phthalate Regulation, and Public Health: A Review. *J. Toxicol. Env. Health-Pt b-Crit. Rev.* **12**, 157-174. <https://doi.org/10.1080/10937400902729226>
- Kreps F, Vrbikova L, Schmidt S. 2014. Influence of industrial physical refining on tocopherol, chlorophyll and beta-carotene content in sunflower and rapeseed oil. *Eur. J. Lipid Sci. Technol.* **116**, 1572-1582. <https://doi.org/10.1002/ejlt.201300460>
- Kong X, Bai Z, Jin T, Jin D, Pan J, Yu X, Cernava T. 2022. *Arthrobacter* is a universal responder to di-n-butyl phthalate (DBP) contamination in soils from various geographical locations. *J. Hazard. Mater.* **422**, 126914. <https://doi.org/10.1016/j.jhazmat.2021.126914>
- Kotowska U, Kapelewska J, Sawczuk R. 2020. Occurrence, removal, and environmental risk of phthalates in wastewaters, landfill leachates, and groundwater in Poland. *Environ. Pollut.* **267**, 115643. <https://doi.org/10.1016/j.envpol.2020.115643>
- Liu JM, Li CY, Zhao N, Wang ZH, Lv SW, Liu JC, Chen LJ, Wang J, Zhang Y, Wang S. 2020. Migration regularity of phthalates in polyethylene wrap film of food packaging. *J. Food Sci.* **85** (7), 2105-2113. <https://doi.org/10.1111/1750-3841.15181>
- Martino-Andrade AJ, Chahoud I. 2010. Reproductive toxicity of phthalate esters. *Mol. Nutr. Food Res.* **54**, 148-157. <https://doi.org/10.1002/mnfr.200800312>
- Mohd AS, Dutta RK, Sen AK. 2018. Removal of diethyl phthalate via adsorption on mineral rich waste coal modified with chitosan. *J. Mol. Liq.* **261**, 271-282. <https://doi.org/10.1016/j.molliq.2018.04.031>
- Net S, Sempere R, Delmont A, Paluselli A, Ouddane B. 2015. Occurrence, Fate, Behavior and Ecotoxicological State of Phthalates in Different Environmental Matrices. *Environ. Sci. Technol.* **49**, 4019-4035. <https://doi.org/10.1021/es505233b>
- Pan FG, Li YY, Luo XD, Wang XQ, Wang CS, Wen BL, Guan XR, Xu YF, Liu BQ. 2020. Effect of the chemical refining process on composition and oxidative stability of evening primrose oil. *J. Food Process Preserv.* **44**, e14800. <https://doi.org/10.1111/jfpp.14800>
- Pang X, Skillen N, Gunaratne N, Rooney DW, Robertson PK. 2021. Removal of phthalates from aqueous solution by semiconductor photocatalysis: A review. *J. Hazard. Mater.* **402**, 123461. <https://doi.org/10.1016/j.jhazmat.2020.123461>
- Pereira J, Selbourne MD, Pocas F. 2019 Determination of phthalates in olive oil from European market. *Food Control* **98**, 54-60. <https://doi.org/10.1016/j.foodcont.2018.11.003>
- Rahardjo AK, Susanto MJJ, Kurniawan A, Indraswati N, Ismadji S. 2011. Modified Ponorogo bentonite for the removal of ampicillin from wastewater. *J. Hazard. Mater.* **190**, 1001-1008. <https://doi.org/10.1016/j.jhazmat.2011.04.052>
- Wang X, Cheng H, Chai P, Bian J, Wang X, Liu Y, Yin X, Pan S, Pan Z. 2020. Pore characterization of different clay minerals and its impact on methane adsorption capacity. *Ene. Fuels* **34** (10), 12204-12214. <https://doi.org/10.1021/acs.energyfuels.0c01922>
- Wei X, Qin G, Jian X, Kailong L, Fengxiang Y, Ting C, Si Q, Can L, Fangbin W. 2020. Cumulative risk assessment of phthalates inedible vegetable oil consumed by Chinese residents *J. Sci. Food Agric.* **100**, 1124-1131. <https://onlinelibrary.wiley.com/doi/epdf/10.1002/jsfa.10121>
- Xiang W, Gong Q, Xu J, Li KL, Yu FX, Chen T, Qin S, Li C, Wang FB. 2019. Cumulative risk assessment of phthalates in edible vegetable oil consumed by Chinese residents. *J. Sci. Food Agric.* **100**, 1124-1131. <https://doi.org/10.1002/jsfa.10121>
- Xiong Y, Zhao ZM, Zhu LP, Chen YT, Ji HB, Yang DP. 2013. Removal of three kinds of phthalates from sweet orange oil by molecular distillation. *Food Sci. Technol.* **53**, 487-491. <https://doi.org/10.1016/j.lwt.2013.04.012>
- Zhang Y, Liang Q, Gao R, Hou H, Tan W, He X, Yu M, Ma L, Xi B, Wang X. 2015. Contamination of Phthalate Esters (PAEs) in Typical Wastewater-Irrigated Agricultural Soils in Hebei, North China. *PLoS ONE* **10** (9), e0137998. <https://doi.org/10.1371/journal.pone.0137998>
- Zhang A, Xiang J, Sun L, Hu S, Li P, Shi S, Fu P, Su S. 2009. Preparation, characterization and application of modified chitosan sorbents for elemental mercury removal. *Ind. Eng. Chem.* **48**, 4980-4989. <https://doi.org/10.1021/ie9000629>
- Zhang T, Wang W, Zhao Y, Bai H, Wen T, Kang S, Song G, Song S, Komarneni S. 2021. Removal of heavy metals and dyes by clay-based adsorbents: From natural clays to 1D and 2D nano-composites. *Chem. Eng. J.* **420**, 127574. <https://doi.org/10.1016/j.cej.2020.127574>

Zhao BB, Gong HD, Li H, Zhang Y, Deng JW, Chen ZC. 2019. Fatty Acid, Triacylglycerol and unsaponifiable matters profiles and physicochemical properties of chinese evening primrose oil. *J. Oleo Sci.* **68**, 719-728. <https://doi.org/0.5650/jos.ess19091>

Zhao ZH, He GX, Peng XY, Lu L. 2014. Distribution and sources of phthalate esters in the top soils of Beijing, China. *Environ. Geochem. Health* **36**, 505-515. <https://doi.org/10.1007/s10653-013-9577-0>